Estimate of X-Ray Shielding and Radiation Monitoring for Safe Operation of the HINS Cavity Test Cave in the Meson Detector Building

Bob Webber

Revised January 2, 2007

The Fermilab High Intensity Neutrino Source (HINS) R&D program is constructing a cavity test cave for RF testing and conditioning of spoke-resonator accelerating cavity structures. Copper (room temperature) cavities and three types of superconducting (SC) spoke resonator structures (ß=0.2, ß=0.4, and ß=0.6) are included in the program. The activity includes both performance assessment of 'first article' cavities and regular conditioning of production cavities. No particles intended for acceleration will be injected into the cavities in the test cave; nevertheless the cavities will be operated at high electric gradients capable of generating x-rays. Quantifying and limiting the electron currents that produce these x-rays is a critical part of the cavity R&D investigation and conditioning process. This note presents an estimate of the x-ray shielding required for full gradient commissioning and operation of these cavity types in this cave.

Assumptions and Estimates

An estimate of the worst case x-ray yield from the cavities must include the maximum energy obtained by electrons emitted from the cavity surfaces, the number of electrons, the power available to drive the electron current, and any physical factors that otherwise limit the electron current.

Electron Beam Energy Assumptions

The cavities to be tested in this cave are all designed for acceleration of non-relativistic particles (hence, the nomenclature ß=0.2, ß=0.4 and ß=0.6). They are inherently inefficient for imparting the full integrated multi-gap cavity voltage to particles of the "wrong" velocity. It is reasonable to assume that the maximum possible energy imparted to an electron in any of these cavities is that of just one accelerating gap rather than the sum of all gaps. The parameters for each of the cavity types to be used for x-ray shielding calculation purposes are shown in Table 1.

Table 1.

Cavity Type	Maximum Total Voltage	# of Gaps	Assumed Electron Beam Energy
Copper	1 MV	2 full and 2 half	0.33 MeV
SC ß=0.2	1.5 MV	2	0.75 MeV
SC ß=0.4	3.5 MV	2	1.75 MeV
SC ß=0.6	9.5 MV	2 full and 2 half	3.2 MeV

Available Electrons

For purposes of shielding calculations, it is assumed that the number of available electrons is not a limiting factor.

Available RF Power

The cavity test cave is served by two RF power transmission lines coupled through appropriate power couplers to a single 325 MHz, 2.5 MW peak power, pulsed klystron capable of a maximum 4.5 msec pulse and 1.5% duty factor. A low-power feed makes available 25 kW peak pulsed power to be used to drive the room temperature, copper cavities. A high-power feed, 250 kW peak, will be used for pulse power testing the superconducting cavities. Maximum average RF power available for electrons for x-ray production is 375 watts (1.5% times 2.5 kW) for the copper cavities and 3750 watts for the superconducting cavities.

Other Physical Factors

The production of x-rays from accelerated electrons is an inefficient process; at energies of concern here >90% of the electron beam power becomes heat in the x-ray producing target [1] [Appendix 1]. For estimating x-ray production by the superconducting cavities, this is important. The superconducting cavities must be maintained at cryogenic temperatures to be operated at design accelerating fields. Any electrons capable of producing x-rays will impinge on and heat the cavity walls or a cavity blank-off flange within the cryostat. In the HINS cavity test installation, the heat that can be removed by the cryogenic system while maintaining a cavity at superconducting temperature is limited to only about 100 watts. It is this cryogenic capacity, not the available RF power that ultimately limits the electron beam power available for x-ray production. For calculations here, it is assumed that 500 watts of electron beam power, limited by cryogenics, not by available RF power, is possible. Choice of 500, rather than 100, watts retains a reasonable safety factor.

Shielding Calculations

Based on assumptions described above, the electron current available for x-ray production from each cavity type is:

Copper cavity	---	375W / 0.33 MV = 1.13 mA
ß=0.2 SC cavity	---	0.5 kW / 0.75 MV = 0.67 mA
ß=0.4 SC cavity	---	0.5 kW / 1.75 MV = 0.29 mA
ß=0.6 SC cavity	---	0.5 kW / 3.2 MV = 0.16 mA

The corresponding absorbed dose rates D for x-rays at one meter from an x-ray producing target are obtained from graph E.1 in NCRP Report No.51.

For copper cavity

At 0° $D = <0.5\ (\text{rad m}^{2)} / (\text{min mA}) \times 1.13\ \text{mA} < 0.6\ \text{rad m}^2/\text{min}$

At 90° $D = 3\ (\text{rad m}^{2)} / (\text{min mA}) \times 1.13\ \text{mA} = 3.4\ \text{rad m}^2/\text{min}$

For ß=0.2 SC cavity

At 0° D = 10 (rad m$^{2)}$ / (min mA) x 0.67 mA = 6.7 rad m^2/min

At 90° D = 30 (rad m$^{2)}$ / (min mA) x 0.67 mA = 20 rad m^2/min

For ß=0.4 SC cavity

At 0° D = 300 (rad m$^{2)}$ / (min mA) x 0.29 mA = 87 rad m^2/min

At 90° D = 150 (rad m$^{2)}$ / (min mA) x 0.29 mA = 44 rad m^2/min

For ß=0.6 SC cavity

At 0° D = 1500 (rad m$^{2)}$ / (min mA) x 0.16 mA = 240 rad m^2/min

At 90° D = 400 (rad m$^{2)}$ / (min mA) x 0.16 mA = 64 rad m^2/min

The most demanding case, the ß=0.6 SC type cavity, is used for the following shielding calculations.

Following Table E.3 in NCRP 51, the dose rates at 0° and 90° can be multiplied by factors of 0.7 and 0.5 respectively for copper/iron production target materials, giving:

At 0° D = 168 rad m^2/min

At 90° D = 32 rad m^2/min

The shielding necessary to limit dose rates to 1 mr/hr (H = 1) outside the shield wall (0° case) and 5 mr/hr on top of the cave roof (90°) is calculated using NCRP 51 equation 4-3.

0° Case:

The SC cavities are mounted horizontally in the test cryostat with the beam line axis along an east-west line. The x-ray source point is taken to be the outer wall of the cavity test cryostat located three feet from the inside wall of the cave. The reference point for shielding calculations is taken to be six feet beyond the inside cave wall for a total ‘distance from source’ parameter d = 9 feet = 2.7 meter. Occupancy factor T = 1 is assumed. From equation 3, NCRP 51, section 4.3.2, find shielding transmission ratio:

$B = 1.67E\text{-}5 * H *d^2 / (D * T) = 1.67E\text{-}5 * 1 * 2.7^2 / 168 = 7.2E\text{-}7$

This attenuation is achieved with n tenth-values layers (TVL) of shielding, where n = log(1/B). In this case, n = 6.1.

For 3.2 MeV x-rays in concrete, the first and subsequent tenth-value layers are each ~10 inches (graph E.12, NCRP 51). Therefore a total wall thickness of 6.4 * 10 = 64 inches will limit the dose rate to <1 mr/hr outside the cave walls.

90° Case:

The x-ray source point is taken to be the axis of the cavity in the test cryostat 50 inches above the cave floor. The cave ceiling height is 15 feet (180 inches). Choosing a reference point 36 inches above the cave ceiling gives d = 166 inches = 4.2 meters. Assume T = 1 and find:

$B = 1.67E\text{-}5 * H * d^2 / (D * T) = 1.67E\text{-}5 * 5 * 4.2^2 / 32 = 4.6E\text{-}5$

To achieve this attenuation n TVLs are required, where n = log(1/B) = 4.3

At the 90° angle, NCRP 51, Table E.6 gives an x-ray spectrum adjustment factor. 3.2 MeV electrons are adjusted to 2 MeV x-rays for shielding calculations. For 2 MeV x-rays in concrete, the first tenth-value layer is ~9 inches and subsequent layers are each ~8 inches. Therefore a roof thickness of 9 + 3.3 * 8 = 35.4 inches will limit the dose rate to <5 mr/hr on the cave roof.

Cave Construction

The cavity test cave is constructed of concrete blocks as shown in plan view in Figure 1.

The 72 inch thick walls, assembled from two overlapping 36 inch concrete blocks, are more than adequate to provide the required 0° shielding. The roof is 36 inches thick, made of overlapping 18 concrete blocks. This offers just the required shielding as calculated.

Figure 2 depicts the cryostat that will be installed in the cave for SC cavity testing.

Proposed Operation

The planned cave wall and roof thicknesses are calculated to be sufficient to allow safe operation of all the proposed cavity types. The ß=0.6 SC cavities present the most demanding case. The first cavity types available for test will be the copper and the ß=0.2 SC cavities for which the shielding offers a generous margin for the x-rays expected. Any discrepancies between actual conditions and the bases of the shielding calculations can be learned from the experience with these first cavities.

Interlocked radiation detectors will be installed at the cave roof and wall to enforce safe operations should radiation rates unexpectedly approach the designated safe limits. These detectors will disable the RF power source when pre-set radiation thresholds are reached.

Additionally, operation under the conditions assumed for estimation of maximum x-ray production rates is inconsistent with the technical and scientific objectives of the cavity testing and conditioning program. Independent of radiation concerns, careful monitoring and limitation of the delivered RF power, cavity heating, and emission currents are required for cavity protection and for qualifying the cavities for accelerator operation at minimum emission currents. The RF power system controls will be configured to facilitate operation at reduced peak power and reduced duty cycle.

Conclusion

The HINS cavity test cave will be constructed with sufficiently thick concrete walls and roof to passively protect personnel from the maximum anticipated x-ray flux from the HINS room temperature copper cavities and superconducting ß=0.2, 0.4, and 0.6 type cavities during testing and conditioning operations. Interlocked detectors capable of disabling the RF power to the cavities will provide an additional level of safety assurance. Normal operation is expected to produce x-rays well below the levels assumed for shielding calculations.

References

1. Evans, Robley D., “The Atomic Nucleus”, McGraw-Hill, 1955, pp. 609-610.

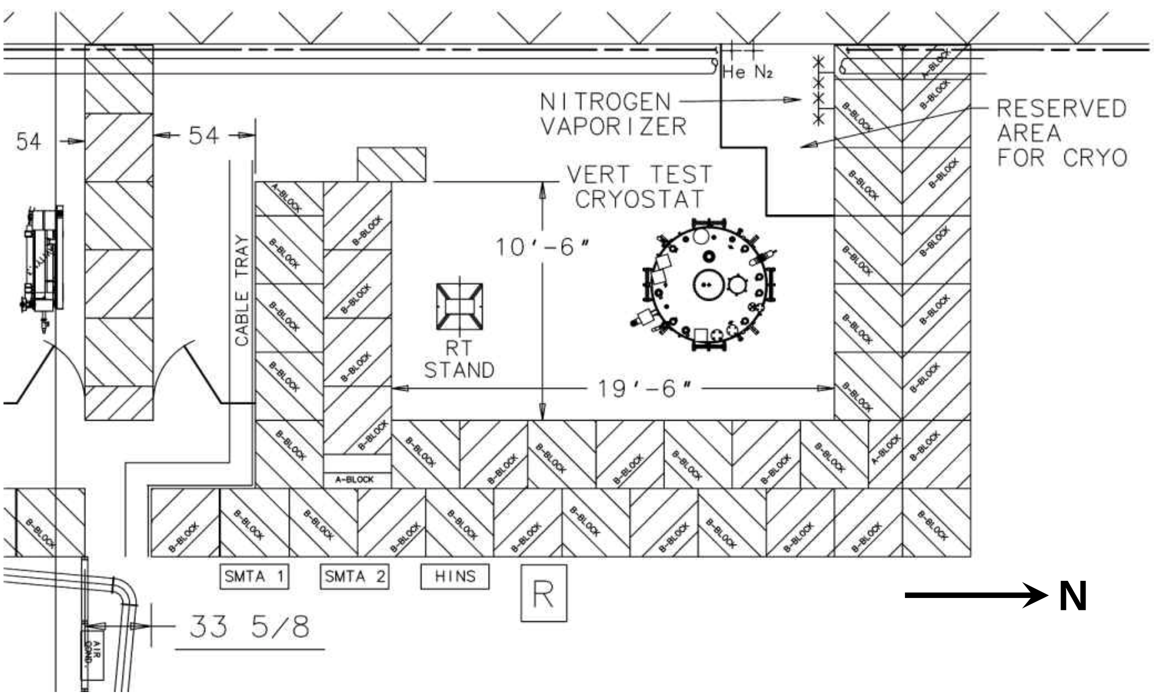

Figure 1. HINS Cavity Test Cave Plan View. Axis of cavity in cryostat is horizontal along East-West line.

Figure 2. SC spoke resonator mounted in test cryostat. View is from west side of cryostat looking to the east along beam axis of cavity.

Appendix 1. From "The Atomic Nucleus", Robley D. Evans

With Webber notations.

THE ATOMIC NUCLEUS

Robley D. Evans, Ph.D.

PROFESSOR OF PHYSICS

MASSACHUSETTS INSTITUTE OF TECHNOLOGY

New York Toronto London

McGRAW-HILL BOOK COMPANY, INC.

1955

The actual path of an electron while passing through an absorbing foil is not straight. Because of the effects of multiple scattering, the actual path length is always greater than the foil thickness traversed. The ratio of the actual path length to the superficial thickness of absorber traversed increases with Z (Chap. 21, Sec. 1). In the case of electrons (but not heavy particles), the effect of scattering almost exactly balances the decrease of dT/dw with increasing Z. Therefore, if distance is measured in terms of superficial thickness of absorber traversed, say, in milligrams per square centimeter, the ionization losses for positrons and

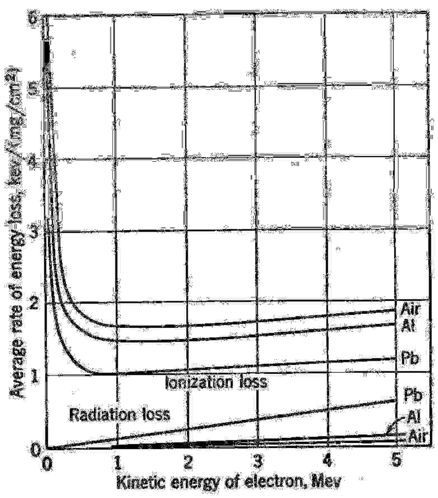

Note: this discussion assumes thin targets

Fig. 2.1 Mass-absorption energy losses for electrons in air, Al, and Pb. The upper three curves are $(dT/dw)_{ion}$, based on Eq. (2.26) of Chap. 18, with $dw = \rho\, ds$, and $I_{air} = 86$ ev, $I_{Al} = 165$ ev, $I_{Pb} = 750$ ev. The three lower curves show, on the same scales, the average energy loss due to bremsstrahlung $(dT/dw)_{rad}$ as obtained from Eq. (1.9), with $dw = \rho\, ds$. All curves refer to energy losses along the actual path traversed by the electron.

negatrons become nearly independent of the nature of the absorbing material. It is therefore common in reporting experimental work to use milligrams per square centimeter, or a similar unit, as the measure of absorber thickness.

c. Ratio of Radiative and Ionization Losses. Ionization losses per unit path length vary roughly as $1/\beta^2$ and so are largest for slow particles. On the other hand, radiative losses increase with increasing energy, Eq. (1.9). At high energies, $T \gg Mc^2$ in general, or $T \gg m_0c^2$ for electrons, the radiative losses become comparable with the ionization losses.

The ratio of the radiative to the ionization losses, for any particle of rest mass M_0, and high velocity $\beta \simeq 1$, is obtainable from the quotient of Eq. (1.9) and Eq. (2.26) of Chap. 18. With $137\sigma_0$ generalized to

$(e^2/M_0c^2)^2$, the ratio becomes approximately (B55)

$$\frac{(dT/ds)_{\text{rad}}}{(dT/ds)_{\text{ion}}} \simeq Z\left(\frac{m_0}{M_0}\right)^2\left(\frac{T}{1{,}600m_0c^2}\right) \tag{2.8}$$

The factor 1,600 holds for electrons ($M_0 = m_0$) but should be reduced to about 1,000 for mesons ($M_0 \sim 200m_0$). Thus we see that, for electrons, the radiative and ionization losses are equal for $T = 20m_0c^2 = 10$ Mev in Pb (and for $T \sim 100$ Mev in water or air).

The numerical values of σ_{rad} are such that *for electrons at 10 Mev the radiative and ionization losses are each equal to about 1.6 Mev per millimeter of Pb*, or a total of 3.2 Mev per millimeter of Pb for both. This makes a very convenient rule of thumb for estimating high-energy radiative losses (which increase approximately with NZ^2 and T) and ionization losses (which increase with NZ but are nearly independent of T).

So for example
with 3 MeV electrons on iron
$Z=26$

$$\frac{\left(\frac{dT}{ds}\right)_{RAD}}{\left(\frac{dT}{ds}\right)_{ION}} = 26\left(\frac{1}{1}\right)^2\left(\frac{T=3\text{ MeV}}{1600(\frac{1}{2}\text{ MeV})}\right)$$

$$= \frac{26\cdot 3}{1600/2} \approx \frac{78}{800} \approx 10\%$$

So at 3 MeV only 10% of electron energy is converted to photons, 90% goes to ionization and therefore to heat in target

For thick targets (series of thin targets w/ ever decreasing electron energy), photon yield is lower yet.